Quaternary Science Reviews 29 (2010) 1107–1115

Contents lists available at ScienceDirect

Quaternary Science Reviews

journal homepage: www.elsevier.com/locate/quascirev

Sub-millennial variability of Asian monsoon intensity during the early MIS 3 and its analogue to the ice age terminations

Dianbing Liu [a], Yongjin Wang [a,*], Hai Cheng [a,b], R. Lawrence Edwards [b], Xinggong Kong [a], Xianfeng Wang [b], Ben Hardt [b], Jiangying Wu [a], Shitao Chen [a], Xiuyang Jiang [a], Yaoqi He [c], Jinguo Dong [a], Kan Zhao [a]

[a] College of Geography Science, Nanjing Normal University, Nanjing 210097, PR China
[b] Department of Geology and Geophysics, University of Minnesota, Minneapolis, MN 55455, USA
[c] The State Laboratory of Environmental Geochemistry, Institute of Geochemistry, Chinese Academy of Sciences, Guiyang 550002, PR China

ARTICLE INFO

Article history:
Received 26 February 2009
Received in revised form
1 January 2010
Accepted 11 January 2010

ABSTRACT

Although the initiation and continuation of orbital and millennial climate transitions were reported to be roughly similar, little is yet known about the extent to which their sequences of climate events are linked together in the same physical processes. Here we present a stalagmite isotope record from Wulu Cave, southwestern China, based on 1200 oxygen isotope data and 15 ^{230}Th ages, registering a detailed history of the Asian Monsoon (AM) from 61.3 to 50.5 ka BP with an average resolution of 12 yr. Two replicated, high-resolution calcite δ^{18}O profiles show four millennial-scale strong summer monsoon events, analogous in timing and structure to Chinese Interstadials A.17–A.14 (CIS A.17–A.14), as recorded elsewhere in China and Greenland Interstadials 17–14 (GIS 17–14). These events exhibit two distinct phases, consistent with multi-decadal/centennial shifts in Greenland temperature and storminess. This relationship reveals a tight coupling between high- and low-latitude climates at sub-millennial scales, implying a role for westerly winds in linking Greenland temperature and the AM. Around the Marine Isotope Stage (MIS) 4/3 boundary, successive AM events resemble, but in higher frequency, structure of the Bølling–Younger Dryas (YD) surrounding Termination I. Along with evidence from similar shifts in bipolar temperature and atmospheric CH_4, we suggest that the recurrence of similar climate structure worldwide is likely caused by changes in Atlantic meridional overturning circulation (AMOC) at various timescales under thresholds of global ice volume boundaries, as predicted by the bipolar seesaw model.

1. Introduction

Marine Isotope Stage 3 (MIS 3), a period of intermediate ice volume, high-latitude summer insolation, and CO_2 concentrations (McManus et al., 1999), was characterized by remarkable stadials/interstadials. Various hypotheses have been proposed as forcing mechanisms behind these extremely rapid climate variations, including Atlantic thermohaline circulation (THC) changes (Broecker et al., 1990; Rahmstorf, 1995), tropical ocean processes (Kudrass et al., 2001; Stott et al., 2002), and external forcing (Munk et al., 2002; Braun et al., 2005; Firestone et al., 2007). However, much remains to be resolved regarding the trigger-response relationship between different climate systems, in part because of limited high-resolution records with sufficient global coverage (Voelker et al., 2002). At the sub-millennial scale, surface temperature over Greenland was reported to shift by 8–15 °C and atmospheric methane (CH_4) changed up to 200 ppb (Huber et al., 2006), indicative of a rapid reorganization of atmospheric circulation. The concentration of calcium ions (Ca^{2+}) in the GISP2 ice core exhibited synchronous changes similar to observed variations in surface temperature (Mayewski et al., 1997), suggesting variability in the atmospheric transport trajectory and moisture conditions of the Ca^{2+} source region, thought to be the Asian continental interior. This may provide insight into a climatic link between high- and low-latitudes, and a potential mechanism for rapid climate changes.

Abrupt climate changes associated with transitions between extreme conditions are ideal for assessing potential forcing mechanisms in the climate system. The onset and temporal evolutionary structure of glacial terminations has been recently suggested to practically parallel those over millennial-scale Antarctic warming (Wolff et al., 2009). If so, the climate system may be coupled at different timescales. Thus, the boundary conditions underlying millennial climate variability should reach a threshold sufficient enough to initiate the deglaciation at terminations, including shifts

* Corresponding author. Tel./fax: +86 25 83598125.
E-mail address: yjwang@njnu.edu.cn (Y. Wang).

0277-3791/$ – see front matter © 2010 Elsevier Ltd. All rights reserved.
doi:10.1016/j.quascirev.2010.01.008

in continental ice volume (Parrenin and Paillard, 2003) and atmospheric carbon dioxide (CO_2) concentration (Indermühle et al., 2000; Ahn and Brook, 2007).

While climate during Terminations I and II (T I and II) has been extensively studied (Alley and Clark, 1999, and the references therein; Wang et al., 2001; de Abreu et al., 2003; Cheng et al., 2006; Kelly et al., 2006), the MIS 4/3 boundary, a shift from glacial to near-interglacial conditions (van Andel, 2002), has received less attention. This period is preceded by an interval of pronounced northern and southern cold, during which the frequently-invoked mechanism of bipolar seesaw (Broecker, 1998) seems to be invalid. Moreover, the MIS 4/3 boundary occurs at a switching point of low- and high-frequency stadial/interstadial cycles (Hinnov et al., 2002), and is appropriate for studying sub-millennial climate variability. Thus, a high-resolution record is needed to further investigate the link of detailed climate events around the MIS 4/3 boundary and glacial terminations.

Whereas Chinese Interstadials 17–14 (CIS A.17–A.14, nomenclature from Cheng et al., 2006) have been identified in earlier Chinese Cave studies (e.g. Wang et al., 2001), here we examine these features at higher resolution (average resolution of 12 years, about 6 years during CIS A.17). We present a record from Wulu Cave, southwestern China, which spans a period from 61.3 to 50.5 thousand years before present (ka BP), allowing a detailed investigation of Asian monsoon (AM) evolution at about the time of the MIS 4/3 boundary. A comparison with the AM variability over T I (Wang et al., 2001; Wu et al., 2009) may facilitate an evaluation of the potential link between the glacial termination and millennial-scale climate transition.

2. Location and sample description

Wulu Cave (26° 03′N, 105° 05′E, 1440 m above sea level) is located in Guizhou, southwestern China (Fig. 1), 290 km northwest of Dongge Cave (Yuan et al., 2004). The Yun-Gui Plateau, a southeastward extension of the Tibetan Plateau, constitutes the main topographical feature of the study site. Situated at the foot of a 50-m-high hill, Wulu Cave is about 800 m long, and overlain by approximately 40 m of Triassic limestone bedrock with a thin soil cover. The cave site is suffered from severe stone desertification and the flora above is mostly composed of deciduous herbs. The cave is poorly ventilated, and measured relative humidity is about 100%. The Yun-Gui plateau is located in a transitional zone between the East Asian and Indian summer monsoons (Wang and Lin, 2002). Local precipitation distinctly increases in late spring as the Indian monsoon intensifies. In summer, regional meteorological conditions are dictated by interactions between the Indian and East Asian summer monsoons. Current mean annual temperature at this site is about 14 °C, with a maximum in July (20.8 °C) and a minimum in January (4.3 °C). The annual precipitation ranges between 1100 mm and 1700 mm, peaking (920 mm) during the summer months (June–September), reaching a minimum (80 mm) in the winter (December–February). Meteorological observations during the last fifty years show that annual precipitation is mainly determined by summer rainfall (with an average percent of 65%), a negligible contribution of less than 8% occurs during the wintertime. Variability of annual rainfall is highly correlated with summer precipitation ($R^2 = 0.62$) (Supplementary Fig. 1).

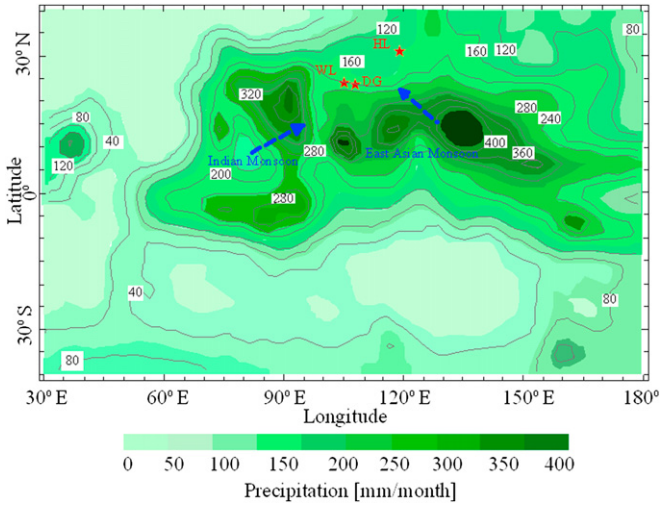

Fig. 1. Global mean August precipitation (mm/month) within the longitudinal and latitudinal ranges of 30°E–180°, 40°N–40°S, including the sites of Hulu Cave (HL, eastern China, 32°30′ N, 119°10′E, Wang et al., 2001), Dongge Cave (DG, southern China, 25° 17′N, 108° 05′E, Yuan et al., 2004) and Wulu Cave (WL, southern China, 26° 03′N, 105° 05′E, this study). Image from the website http://ingrid.ldgo.columbia.edu/. The numbers in the figure show the monthly rainfall, and the two thick, dashed arrows denote the Indian and East Asian monsoon subsystems.

The two stalagmites, Wu23 and Wu26, were collected 5 m apart and 650 m from the entrance. Sample Wu23 is 66.7 cm in length (Supplementary Fig. 2). It has a 'candlestick' shape and a diameter of ~6.5 cm, indicating a stable deposition history. Sample Wu26 is 83 cm long and has a larger diameter, varying from ~9 cm to 10 cm. When halved and polished, couplets of faint transparent/dark layers are apparent from 52 cm to 81.6 cm depth in Wu26. At 25 cm, 41 cm and 50 cm, changes in color suggest a growth cessation or changes in the growth rate at these depths. In Wu23, black organic-rich bands are evident at a depth of 8 cm, indicative of a growth hiatus. At 36 cm, horizontal bands are gradually replaced by curved ones in this sample, suggesting a shift in moisture conditions and/or growth rate.

3. Analytical methods

Fifteen calcite powder samples were drilled along the growth axis of stalagmites (six for Wu23 and nine for Wu26) with 0.9 mm-diameter carbide dental burrs for ^{230}Th dating. The measurements were performed by inductively coupled plasma mass spectrometry (ICP-MS) on a Finnigan-MAT Element at the Department of Geology and Geophysics, University of Minnesota, USA. The procedures are similar to those described in Shen et al. (2002), with results listed in Table 1. All dates are in stratigraphic order with typical analytical errors (2σ) ranging from 130 to 400 yr. For stable isotopic measurements, 1200 sub-samples were drilled with 0.3 mm-diameter carbide dental burrs along the growth axis. Analyses were performed on a Finnigan-MAT 253 mass spectrometer fitted with a Kiel Carbonate Device at the College of Geography Science, Nanjing Normal University. Spatial resolution is 0.5–1 mm for Wu23 and 1–2 mm for Wu26. This corresponds to a temporal resolution of 2 yr–40 yr for different portions of the two samples. The results were reported relative to Vienna PeeDee Belemnite (VPDB) with standardization determined relative to NBS 19. Precision of $\delta^{18}O$ values is 0.06‰, at the 1-sigma level.

4. Results

4.1. U/Th chronology

Fifteen ^{230}Th dates reveal that the growth of two stalagmites covers a period from 61.3 ± 0.26 to 27 ± 0.13 ka BP (Table 1), with most of the deposition occurring in the early MIS 3 (from 61.3 to 50.5 ka BP). These dated calcite powders have high uranium (400–710 ng/g) and relatively low thorium concentrations

Table 1
^{230}Th dating results for two stalagmites from Wulu Cave, southwestern China.

Sample number	Depth (cm)	^{238}U (ng/g)	^{232}Th (pg/g)	δ^{234}U (measured)	^{230}Th/^{238}U (activity)	^{230}Th age (yr BP) (Uncorrected)	^{230}Th age (yr BP) (Corrected)	$\delta^{234}U_{Initial}$ (Corrected)
Wu23-11	1.1	620 ± 1	211 ± 3	1384 ± 4	0.533 ± 0.002	26980 ± 130	**26970 ± 130**	1494 ± 5
Wu23-100	10.0	500 ± 1	347 ± 3	1311 ± 4	0.964 ± 0.003	55750 ± 260	**55740 ± 260**	1534 ± 5
Wu23-261	26.1	405 ± 1	488 ± 15	1371 ± 3	1.014 ± 0.004	57370 ± 310	**57360 ± 310**	1611 ± 4
Wu23-373	37.3	443 ± 1	165 ± 2	1331 ± 5	1.010 ± 0.004	58430 ± 290	**58430 ± 290**	1570 ± 6
Wu23-480	48.0	530 ± 1	327 ± 13	1320 ± 4	1.020 ± 0.005	59470 ± 390	**59470 ± 390**	1561 ± 4
Wu23-645	64.5	596 ± 1	204 ± 3	1293 ± 4	1.011 ± 0.003	59810 ± 250	**59800 ± 250**	1531 ± 4
Wu26-54	5.4	711 ± 1	3855 ± 7	1273 ± 4	0.890 ± 0.003	51630 ± 220	**51560 ± 220**	1473 ± 5
Wu26-149	14.9	636 ± 1	421 ± 8	1240 ± 2	0.903 ± 0.001	53460 ± 120	**53450 ± 120**	1442 ± 3
Wu26-238	23.8	628 ± 1	411 ± 3	1249 ± 4	0.915 ± 0.003	54110 ± 260	**54110 ± 260**	1455 ± 5
Wu26-259	25.9	479 ± 1	295 ± 3	1276 ± 4	0.936 ± 0.004	54840 ± 290	**54830 ± 280**	1489 ± 5
Wu26-430	43.0	434 ± 1	322 ± 6	1256 ± 2	0.962 ± 0.001	57270 ± 130	**57260 ± 130**	1476 ± 3
Wu26-490	49.0	581 ± 1	342 ± 3	1271 ± 4	0.974 ± 0.003	57720 ± 280	**57710 ± 280**	1497 ± 5
Wu26-526	52.6	556 ± 1	107 ± 3	1258 ± 4	0.990 ± 0.004	59400 ± 300	**59400 ± 300**	1488 ± 5
Wu26-663	66.3	522 ± 2	182 ± 6	1280 ± 6	1.011 ± 0.005	60120 ± 400	**60120 ± 400**	1517 ± 7
Wu26-817	81.7	646 ± 1	445 ± 3	1247 ± 4	1.008 ± 0.003	61200 ± 260	**61190 ± 260**	1482 ± 5

Errors are 2σ analytical errors. Decay constant values are $\lambda_{230} = 9.1577 \times 10^{-6}$ yr^{-1}, $\lambda_{234} = 2.8263 \times 10^{-6}$ yr^{-1}, $\lambda_{238} = 1.55125 \times 10^{-10}$ yr^{-1}. Corrected ^{230}Th ages assume an initial ^{230}Th/^{232}Th atomic ratio of $(4.4 \pm 2.2) \times 10^{-6}$. Corrected ^{230}Th ages are indicated in bold.

(110–490 pg/g). Thus, initial ^{230}Th age corrections are trivial (generally less than 15 yr), ensuring high-precision dating results. The two stalagmites are closely situated, and influenced by similar climatic and edaphic conditions. A considerable discrepancy of corrected $\delta^{234}U_{Initial}$ values (an indicator of the ratio of excess ^{234}U to ^{238}U in the seepage water when calcite deposited) observed between them might have little climatic/edaphic origin. One possibility is due to different types of conduit feeding two stalagmites and associated water–rock interactions (Kaufman et al., 1998), which is clearly reflected in their different diameters.

An age model was developed for the stable isotope data by linear interpolation between ^{230}Th dates. One age in Sample Wu23 (26,970 ± 130 yr BP) was above an apparent hiatus and was not used in constructing the age model. Below the hiatus, growth rate ranges from 100 mm/ka to 660 mm/ka (Fig. 2). Between 52 and 81.6 cm depth of Wu26, an average of 4–5 couplets of light/dark layers can be identified per millimeter. If these are annual bands, they would indicate a growth rate of 200–250 mm/ka (Supplementary Fig. 2), which agrees reasonably well with our estimate of 163 mm/ka from the bounding U/Th dates (59,400 ± 300 yr BP; 61,190 ± 260 yr BP). The growth periods for two samples overlap each other from 59.8 to 55.5 ka BP, with a discontinuity in Wu26 from 59.4 to 57.7 ka BP.

Sample Wu23 (Supplementary Fig. 2) exhibits little variability in lithological features below the hiatus at 8 cm, leading to a near-linear age model over the large interval and a slight shift in the growth rate at a depth of 48 cm (Fig. 2). Occasional changes in lithology above the depth of 50 cm in Sample Wu26 may account for large variation of growth rate estimated by a linear interpolation between dates, ranging between 20 mm/ka and 130 mm/ka. Below this depth the age model is practically linear. Consequently, the age model we established from an interpolation between two dating points is roughly supported by the observed lithological variations.

4.2. Isotopic equilibrium fractionation test

Equilibrium calcite precipitation is a prerequisite for the applicability of calcite $\delta^{18}O$ ($\delta^{18}O_{calcite}$) to paleoclimate reconstruction. A correlation test between $\delta^{18}O$ and $\delta^{13}C$ (Supplementary Fig. 3) for each sample reveals a weak relationship ($R^2 = 0.07$ for Wu23, 0.003 for Wu26), that is not statistically significant. 'Hendy tests' (Hendy, 1971) performed on seven growth lamina (four for Wu23, three for Wu26) show little variability in $\delta^{18}O$ values within a radius of ~3 cm from the central axis (indicated by 0 cm in Supplementary Fig. 3) to the edges, with a standard deviation less than 0.23‰ along each layer. In contrast, $\delta^{13}C$ values shift by 0.7–2.6‰ along these same layers. A potential interpretation for these observed large $\delta^{13}C$ changes is different CO_2 degassing rate at the stalagmite surface (Romanov et al., 2008) and/or errant sampling beyond the targeted growth layer, which more substantially impacts calcite $\delta^{13}C$ than $\delta^{18}O$ (Mickler et al., 2006). These results indicate that calcite most likely precipitated under equilibrium conditions, although a kinetic effect on the deposited calcite is not currently excluded for lack of

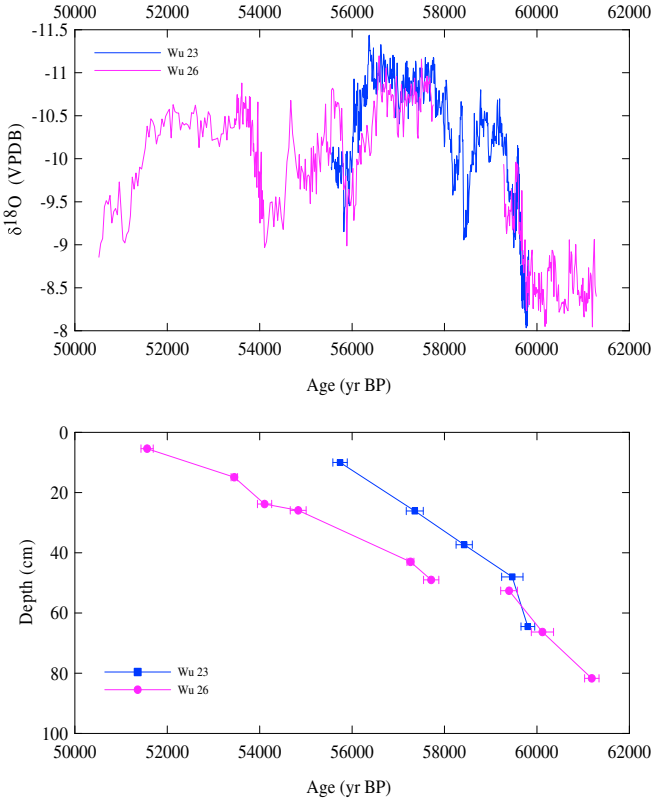

Fig. 2. $\delta^{18}O$ profiles of Samples Wu23, Wu26 and their growth rates. Upper panel: Wu23 $\delta^{18}O$ (blue curve), Wu26 $\delta^{18}O$ (pink curve). Lower panel: the growth rates for two samples. To clearly reveal their contemporaneous variations, the $\delta^{18}O$ values and growth rate for Sample Wu23 younger than 50 ka BP are not shown.

sufficient monitoring work. Due to increasing insufficiency of Hendy criterion in testing calcite equilibrium deposition (Dorale and Liu, 2009), we further perform a replication test. Virtually identical fluctuations of $\delta^{18}O$ from the two stalagmites within Wulu Cave (Fig. 2) and other cave records in China (Wang et al., 2001; Yuan et al., 2004) over contemporaneous growth periods provide an appreciable confirmation for equilibrium calcite deposition. This implies that the $\delta^{18}O$ signal is primarily of climatic origin and that kinetic fractionation has little effect. Thus, variations in $\delta^{18}O_{calcite}$ can be interpreted to reflect changes in cave temperature and/or the isotopic composition of precipitation (Hendy, 1971).

Temperature is unlikely to be a major control on $\delta^{18}O_{calcite}$ variation as that would require a temperature shift of more than 15 °C due to water-calcite temperature-dependent fractionation (−0.23‰/°C, Kim and O'Neil, 1997). Modern meteorological observations reveal that summer precipitation is the largest contributor to annual rainfall at the studied site (Supplementary Fig. 1), and thus seepage water in the cave. The observed isotopic composition of precipitation from a nearby meteorological station (Guiyang, 26°35′N, 106°43′E; elevation = 1071 m, 190 km NE of Wulu Cave) indicates a clear seasonal signal (IAEA/WMO, 2001). Mean values of precipitation $\delta^{18}O$ are lower (average ~ −9.93‰, VSMOW) during the summer than during the winter (average ~ −4.26‰, VSMOW) (Supplementary Fig. 4). Therefore, we propose that $\delta^{18}O_{calcite}$ largely represents regional precipitation change, an indicator of summer monsoon intensity (Wang et al., 2001; Yuan et al., 2004; Cheng et al., 2006).

4.3. Stable isotope sequence

$\delta^{18}O_{calcite}$ values from two samples vary within a total range of 3‰ (from ~ −8.1‰ to −11.1‰) (Fig. 2). Abrupt (sub-millennial) shifts have amplitudes as high as ~1.8‰, more than half the total observed magnitude. Multi-decadal to centennial shifts in $\delta^{18}O$ values range from ~0.7‰ to 1‰. The two $\delta^{18}O$ profiles are characterized by five abrupt shifts to higher $\delta^{18}O$ values, centered at 59.5, 58.5, 58.2, 55.9, and 54.1 ka BP (Note that Fig. 2 has increasing $\delta^{18}O$ plotted downward). Three additional shifts, though smaller in magnitude (averaging ~0.7–1‰), are evident at 59, 57, and 55 ka BP. The growth of Wu23 and Wu26 ceased at 55.5 ka BP and 50.5 ka BP, respectively. After a long cessation, the deposition of stalagmite Wu23 resumed, but only lasted for several hundred years, centering at 27 ka BP.

Our composite $\delta^{18}O$ profile (Fig. 3a) exhibits remarkable similarity to the records from Hulu and Dongge caves (Wang et al., 2001; Yuan et al., 2004), with $\delta^{18}O$-depletion events between records matching within their dating errors. Wulu Cave lies about 1500 km southwest of Hulu Cave and 290 km northwest of Dongge Cave, and all three sites are influenced by the AM. Millennial shifts in the previous cave $\delta^{18}O$ records have been interpreted to broadly reflect changes in $\delta^{18}O$ values of meteoric precipitation (Wang et al., 2001; Yuan et al., 2004), and in turn, relate to changes in the AM intensity. The resemblance of cave $\delta^{18}O_{calcite}$ records from these three sites indicates that isotopic composition of AM precipitation is, at least, regionally similar on millennial-scales.

5. Discussion

5.1. Synchroneity of sub-millennial changes in Greenland temperature and AM intensity

The well-defined patterns of the composite $\delta^{18}O_{calcite}$ sequence are reminiscent of warm episodes in Greenland, e.g. Greenland Interstadial (GIS) 17–14. These four strong monsoon events (CIS A. 14, to A, 17), constrained by 14 ^{230}Th dates, last 2670 ± 340 yr, 1140 ± 390 yr, 2340 ± 390 yr, 1050 ± 380 yr, respectively. Their lengths are roughly supported by the annual layer counting chronology (GICC05) of NGRIP record (2560 ± 160 yr, 920 ± 60 yr, 1780 ± 100 yr, 880 ± 60 yr, Svensson et al., 2008) and GISP2 timescale (~1940 yr, 1110 yr, 2170 yr, 1100 yr, with a counting error of 10%, Meese et al., 1997) within their dating uncertainties. A slightly larger difference (560 yr) between GICC05 timescale and our ^{230}Th age observed during Interstadial 16 is possibly caused by an abrupt shift of growth rate in our age model.

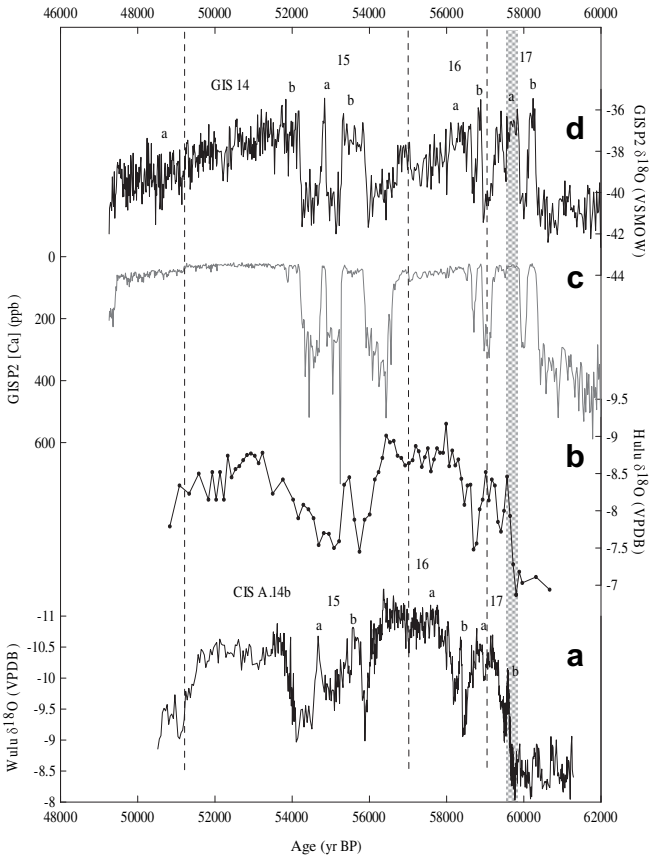

Fig. 3. (a) Oxygen isotopic record from Wulu Cave (this study). (b) $\delta^{18}O$ record from Hulu Cave (Wang et al., 2001). (c) Calcium ion concentration from GISP2 ice core (Mayewski et al., 1997). (d) $\delta^{18}O$ profile from GISP2 ice core (Stuiver and Grootes, 2000). All records are plotted on their respective time scales. Note that Profiles c and d are plotted on the topmost time axis, the other curves are drawn on the bottom time axis. GIS indicates Greenland interstadial, CIS A. depicts Chinese interstadial during the Last Glacial. The numbers show the millennial-scale warming/wetting events in Greenland and the Asian continental interiors, and the letters label the sub-cycles. The dashed lines illustrate the cold/dry events during the interstadials, and the vertical grey bar indicates the MIS 4/3 transition. To aid comparison, Profile c is drawn on a reversed vertical axis.

CIS A.15 in our record, spanning a thickness of 6.9 cm (Supplementary Table 1), is clearly marked by the same 'double-spike' pattern observed in the GISP2 ice record (Fig. 3, Stuiver and Grootes, 2000). The aridity event between the doublets however appears less intense than the corresponding cold event in the Greenland ice cores. Not only does CIS A.15 resemble GIS 15 in the ice core $\delta^{18}O$ ($\delta^{18}O_{ice}$) records, it also inversely correlates to the wind-borne Ca^{2+} record (Fig. 3, Mayewski et al., 1997). Unambiguous peak-to-peak correlation between Greenland temperature and AM intensity persisted throughout the early part of MIS 3. This suggests that, on sub-millennial scales, the Asian continental interior underwent measurable changes in monsoon intensities, with wetter conditions coinciding with Greenland warming and decreased storminess over the high northern latitudes.

During MIS 3, the Chinese and Greenland records are both characterized by sub-millennial variability. We can thus test for their sub-millennial-scale links. GIS 14 is characterized by two peaks, bifurcated by a noticeable cooling (indicated by the dashed line in Fig. 3). Due to a depositional hiatus, CIS A.14 in Wulu Cave record does not include the full interstadial. The existing strong monsoon event is, in terms of pattern and duration, consistent with the older sub-cycle of GIS14 (14b), a relationship also observed in another stalagmite from Austria (Spötl et al., 2006). Similarly, CIS A.16 in Wulu $\delta^{18}O_{calcite}$ exhibits a sharp intensification in the AM and a long period of persistent strong monsoon, consistent with GIS 16b and 16a. The initial jump in AM intensity ($\sim$1.6‰/60 yr in $\delta^{18}O_{calcite}$) is analogous to the abrupt warming in Greenland ($\sim$5‰/40 yr in $\delta^{18}O_{ice}$). Multi-decadal oscillations are evident in $\delta^{18}O_{calcite}$ and $\delta^{18}O_{ice}$ records over Interstadial 16a, with a strong AM event (at 56.4 ka BP) consistent in structure with an abrupt warming in GISP 2 record (at 54.9 ka BP) near the end. The Ca^{2+} record (Fig. 3, Mayewski et al., 1997) displays a general pattern similar to the sub-cycles of CIS A.16, with minimum calcium concentrations during periods of strong summer monsoon. Two remarkable sub-cycles for Interstadial 17 are observed in both Greenland and our cave $\delta^{18}O$ records, with a measurable cooling/drying event punctuating Interstadial 17a (Fig. 3). This interstadial in the cave record, with a thickness of $\sim$26 cm and an average resolution of 6 yr, provides detailed information about monsoon variability over this period.

At the onset of Interstadial 17, an abrupt increase in monsoon intensity, indicated by a decrease of $\sim$2‰ in 200 yr in $\delta^{18}O_{calcite}$ (Fig. 4), shows a strong resemblance to the sharp warming over Greenland ($\sim$5‰ in about 170 yr in GISP2 $\delta^{18}O_{ice}$). Furthermore, in Sample Wu 26, a total thickness of 39 mm and an annual layer counted growth rate of 4–5 couplets/mm (discussed in Section 4.1) define a duration of $\sim$160–200 yr for this AM shift (Supplementary Fig. 2), which agrees well with an estimate of 200 yr based on ^{230}Th ages. These observations are also consistent with storm intensity variability over Greenland (Mayewski et al., 1997). Four centennial, low-amplitude (0.7–0.9‰) oscillations occur during the initial growth period, similar to fluctuations observed in the GISP2 $\delta^{18}O$ record (Fig. 3).

Our comparison reveals that AM variations are intimately linked to Greenland temperature and storm intensity. This close coupling implies a sensitivity of broad areas of the ocean-atmosphere system to abrupt shifts between climate states when climate is near tipping points. The multi-decadal to millennial correlation between Wulu Cave $\delta^{18}O_{calcite}$ and GISP2 Ca^{2+} records (Mayewski et al., 1997) suggests that periods of strong Asian summer monsoon correlate with low storm activity over Greenland, for example, during CIS A.17b, A.16b and A.15. Ca^{2+} variability reflects changes in both transport conditions to Greenland and terrestrial source strength (likely in Asian drylands, Svensson et al., 2000; Ruth et al., 2007). Large dust outbreaks coincide with strong winter monsoon winds in spring (Bory et al., 2002), possibly tied to the strength of the westerlies (Porter and An, 1995). Assuming that stadials/interstadials are synchronous in Greenland and China, these observations support the idea that the strength of the Asian winter monsoon may be inversely correlated to variability in the summer monsoon at multi-decadal to millennial-scales (Yancheva et al., 2007) during the early part of MIS 3, although relatively low concentrations of Ca^{2+} can be observed during the Younger Dryas (YD) and Heinrich event 1 (H1) (Mayewski et al., 1997).

It has been proposed that Atlantic Meridional Overturning Circulation (AMOC) may provide a trigger for millennial-scale climate variability (Broecker et al., 1990; Rahmstorf, 1995) and interhemispheric coupling (EPICA Community Members, 2006). However, the striking similarity of abrupt wetting (warming)/drying (cooling) switches identified for Greenland temperature and AM intensity suggest rapid transmission through the atmosphere. If the wind field is of primary importance in linking different climate systems (Mikolajewicz et al., 1997; Wunsch, 2006; Brauer et al., 2008), a shift in THC associated with variability in the extent of sea ice (Vidal et al., 1998; Li et al., 2005) is likely to be tightly linked to low-latitude changes in hydrological and thermal conditions (Schmittner et al., 2000; Latif, 2001; Hoerling et al., 2001; Stott et al., 2002). Similar relationships have been noted in changes of the El Niño/Southern Oscillation (Timmermann et al., 2007) and latitudinal migration of the Intertropical Convergence Zone (Vellinga and Wood, 2002; Broccoli et al., 2006), phenomena closely related to AM variations (Wang et al., 2004, 2007). Further investigation of high-resolution NGRIP ice core data suggest that AM intensity was synchronous with Greenland warming on the decadal scale (Steffensen et al., 2008), suggesting a tight coupling between the tropical ocean and the moisture-source region for Greenland snow. This multi-decadal link between the AM and Greenland temperature is supported by our record.

5.2. The MIS 4/3 transition analogous to glacial termination

Wolff et al. (2009) suggested that the initiation and subsequent warming into glacial terminations are analogous in structure to millennial-scale Antarctic Isotopic Maximum (AIM) events. This idea points to an important feature of the climate system that climate changes at various temporal scales might reoccur in a similar fashion. In other words, multi-scale and multi-level boundary conditions can nonlinearly conspire to produce comparable oscillations in the climate system under appropriate circumstances (Ganopolski and Ramstorf, 2002). The observed consistency between orbital and millennial climate variability (Wolff et al., 2009) thus highlights a crucial capability of cyclic self-adjustment for the climate system. Motivated by his idea, here we seek to investigate the degree of similarity of detailed climate sequences between the MIS 4/3 transition and T I though the parallel evolution was revealed by Wolff et al. (2009).

The AM variability in the MIS 4/3 time window (Fig. 4b), with a characteristic of glacial terminations, proceeded from similar baseline values as during T I (Fig. 4a), i.e. the weak monsoon during MIS 4 and the Last Glacial Maximum (LGM). After that, the AM evolution at T I was punctuated by two weak monsoon intervals (H 1 and YD) interpolated with a 1800-yr interstadial (Bølling-Allerød, B-A) (Wang et al., 2001; Wu et al., 2009) (Fig. 4a). The total duration from B-A to YD is about 3000 yr (from 14.6 ka BP to 11.6 ka BP). The strengthening of AM to highest-level at the MIS 4/3 boundary is highly consistent, in trend, amplitude and structure, with the T I except for a shorter duration (1600 yr from 59.6 ka BP to 58 ka BP). Following the terminology for the T1, we re-defined sequence of events between CIS A.17 and 16b as Bølling-Allerød at MIS 4/3 (B-A-4/3) and Younger Dryas at MIS 4/3 (YD-4/3) (Fig. 4b). We further observed a more detailed similarity, including internal oscillations during the B-A and one reversal during YD. The resemblance implicates a common forcing mechanism behind the sequence of events during the AM MIS 4/3 transition and T I.

The similar structure seems to be pervasive worldwide as it also appears in temperature and CH_4 records from two polar ice cores. It is not in double that the highest resolution CH_4 data from the NGRIP (Huber et al., 2006) display an extreme similarity to the monsoon record as the two records are mechanistically linked together as discussed in Chappellaz et al. (1993). Temperature changes at Greenland, which proceeded as a similar variation of atmospheric CH_4 concentration, therefore, can be termed as the B-A-YD-4/3 from 59.6 ka BP to 58.6 ka BP (Svensson et al., 2008; Fig. 4). It is difficult to assess the similar structure for Antarctic

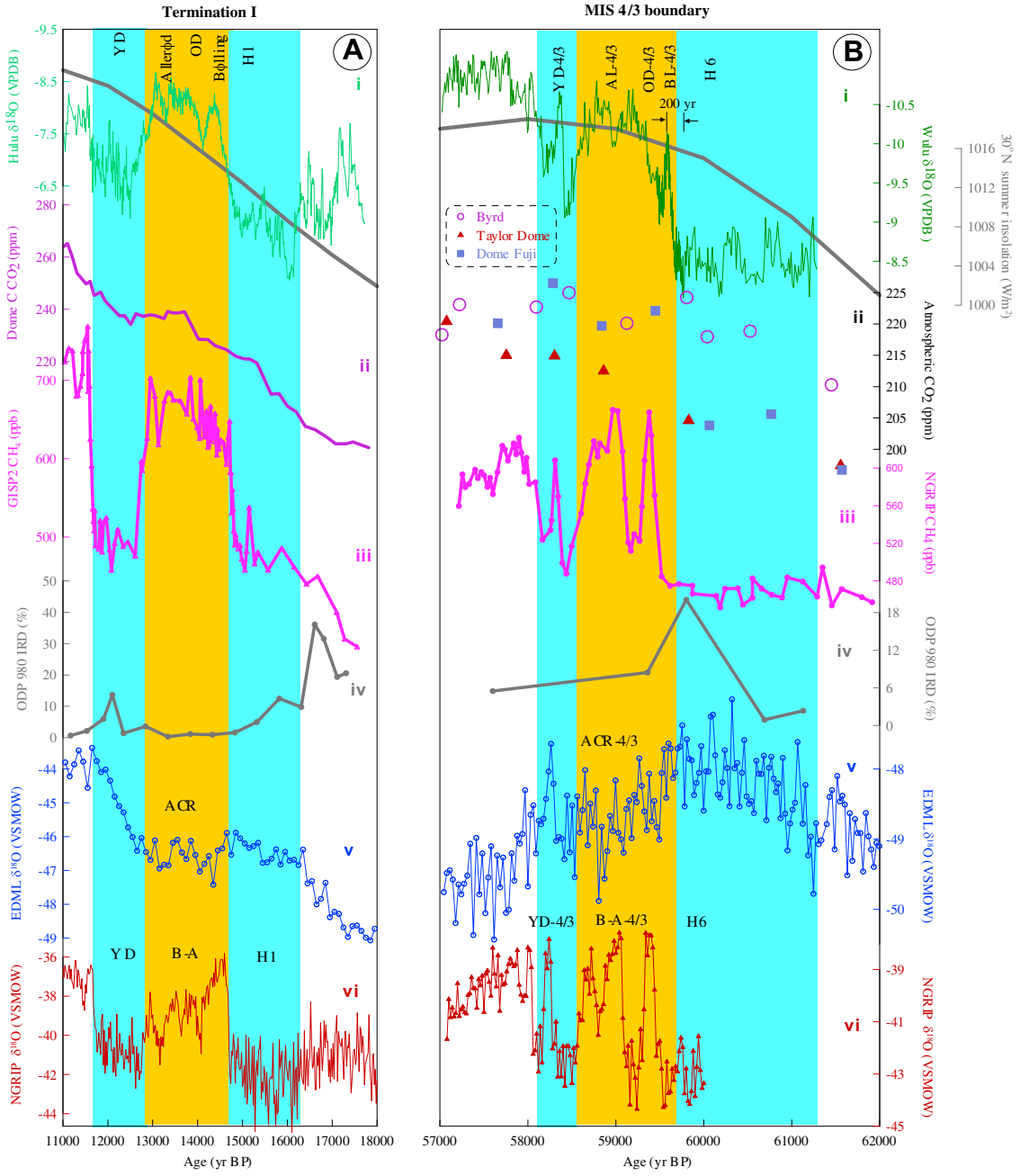

Fig. 4. Major events surrounding (A) Termination I and (B) the MIS 4/3 boundary. Panel A: (i) H82 $\delta^{18}O$ from Hulu Cave (light green curve, Wang et al., 2001; Wu et al., 2009) and July 21 insolation at 30° N (grey line, Berger, 1978). (ii) Antarctic atmospheric CO_2 record from Dome C ice core (Monnin et al., 2001). (iii) GISP2 CH_4 record (Blunier and Brook, 2001). (iv) Ice-rafted debris peaks at ODP Site 980 (McManus et al., 1999). (v) EDML $\delta^{18}O$ (EPICA Community Members, 2006). (vi) NGRIP $\delta^{18}O$ (Svensson et al., 2008). Panel B: (i) Wulu $\delta^{18}O$ (light green, this study) and July 21 insolation at 30° N (grey line, Berger, 1978). (ii) Atmospheric CO_2 from Antarctic ice cores (solid triangles from Taylor Dome, Indermühle et al., 2000; solid squares from Dome Fuji, Kawamura et al., 2003; open circles from Byrd, Ahn and Brook, 2007). (iii) NGRIP CH_4 (Huber et al., 2006) plotted on GICC05 chronology. (iv) Ice-rafted debris peaks at ODP Site 980 (McManus et al., 1999). (v) EDML $\delta^{18}O$ (EPICA Community Members, 2006), which is synchronized to our ^{230}Th age by shifting the ED3 timescale 1000 years older. (vi) NGRIP $\delta^{18}O$ (Svensson et al., 2008). The equivalent AM events around two climate transitions are indicated by color bars and labeled at the topmost. YD, OD, H1 and ACR are abbreviations for Younger Dryas, Older Dryas, Heinrich event 1 and Antarctic Cold Reversal. YD-4/3, AL-4/3, OD-4/3, BL-4/3, ACR-4/3 and H6 represent Younger Dryas, Allerød, Older Dryas, Bølling, Antarctic Cold Reversal and Heinrich event 6 at MIS 4/3 transition, respectively. The vertical lines in Panel B (i) illustrate an abrupt intensification in the AM at MIS 4/3 boundary, lasting ~200 yr.

temperature changes as they show different evolution trends between T I and MIS 4/3. As in EDML $\delta^{18}O_{ice}$ record (EPICA Community Members, 2006), a persistent increase in Antarctic temperature during the Last Deglaciation is punctuated by an Antarctic Cold Reversal (ACR in Fig. 4a) that can be analogous to a comparable cold event (ACR-4/3 in Fig. 4b) during the early MIS 3. But its total length is about half of that during ACR and superimposed on a long-term decreased trend in Antarctic temperature record. Therefore, changes in bipolar temperatures are also anti-phase related at finer scales at MIS 4/3. These similar structures observed between T I and MIS 4/3 transition indicate the climate system can be coupled at different timescales, which supports the notion of a prevalent phenomenon of self-similarity inherent to the climate system (Wolff et al., 2009).

Changes in insolation (Berger, 1978) have been proposed to be a primary control for glacial/interglacial climate variability. But solar insolation can not be considered to interpret the discrepancy of detailed AM sequences around T I and II (Wang et al., 2001; Cheng et al., 2006), suggesting that other factors that trigger the similar sequence of events arose likely from the Earth system, such as changes in ice-sheets, reorganization of oceanic/atmospheric circulations. The most plausible factor would be oceanic thermohaline circulations as the observed anti-phase relationship between two hemispheres can well be explained with bipolar seesaw model (Broecker, 1998). Indeed, the two IRD events (H 1 and H 6) are separately prior to the two analogous sequences of events during T I and MIS 4/3 (Hemming, 2004), although they are from different provenances and little is precisely known about the freshwater flux for the later. This suggests an important role of AMOC in driving global millennial-scale changes. However, the IRD event that triggered the YD-4/3 has not been found yet.

The two periodicities (~3000 yr for T I and ~1600 yr for MIS 4/3) identified for the two transitions were observed in the IRD events in North Atlantic during the late of the Last Glacial periods (Bond and Lotti, 1995). This suggests that meltwater flux at higher frequency band (1600 yr) likely occurred during the early MIS 3. Changes in AMOC strength at finer timescales, from decadal to centennial, have been detected by simulation models and observations (Sy et al., 1997; Marshall et al., 1998; Goodman, 2001; Dickson et al., 2002; Otterå et al., 2003). The changes in AMOC at shorter timescales should be a physical mechanism that can explain our observed AM variations at MIS 4/3 that are in-phase related to CH_4 and Greenland temperature and anti-phase related to Antarctic temperature changes (Fig. 4). Modeling work has suggested that frequency of freshwater discharges into the North Atlantic associated with thresholds of ice volume size can induce self-sustained oscillations of the large-scale ocean circulation (Sima et al., 2004). Geologic records revealed large retreats of continental ice sheet during the early MIS 3 (Svendsen et al., 2004) and the Last Deglaciation (Rinterknecht et al., 2006; Carlson et al., 2008), potentially resulting in rejuvenation of the AMOC activity and ice-free, warm as present-day conditions in northern Scandinavia (Helmens et al., 2007), consistent with modeling result (Sima et al., 2004). Thus, they may favor re-activation of ocean circulations in a similar way that can account for the parallel structures observed around T I and MIS 4/3 transition. As the atmospheric CO_2 fluctuations across the two transitions (~80 ppm for T I, 30 ppm for MIS 4/3) have a similar increase trend (Fig. 4, Indermühle et al., 2000; Blunier and Brook, 2001; Monnin et al., 2001; Kawamura et al., 2003; Ahn and Brook, 2007), CO_2 feedbacks to the AMOC changes (Liu et al., 2009) may contribute to the similar sequence of climate events at T I and MIS 4/3, but its physical processes requires further investigation.

6. Conclusions

Two ~12-yr resolution $\delta^{18}O$ records from Wulu Cave, southwestern China, constrained by 15 ^{230}Th dates, provide the highest resolution record of AM variability during the early MIS 3. The $\delta^{18}O$ profiles are characterized by four distinct wetting/drying cycles from CIS A.17 to CIS A.14. This climate pattern, broadly resembling other cave records from China (Wang et al., 2001; Yuan et al., 2004), appears to correlate with multi-decadal to millennial changes in Greenland temperature (Stuiver and Grootes, 2000) and the general pattern of the wind-borne calcium ion record in the ice (Mayewski et al., 1997).

Our independently dated Wulu records provide the necessary resolution and age certainty to investigate the observed link between high- and low-latitude climates at sub-millennial scales. The comparison with the calcium ion record from Greenland ice (Mayewski et al., 1997) suggests that the Asian summer monsoon is likely anti-phased with the winter monsoon on multi-decadal to millennial-scales (Yancheva et al., 2007).

Furthermore, the detailed AM variability around MIS 4/3 boundary exhibits a strong resemblance, in trend, pattern and magnitude, to that surrounding T I (Wang et al., 2001; Wu et al., 2009). The similar structure also appears in bipolar temperature and atmospheric CH_4 records, which can be explained by bipolar seesaw hypothesis with a physical model of AMOC changes. Different frequency variability of AMOC under certain threshold of the glacial boundary can predispose the climate to free oscillations and behave a self-similarity mode (Ganopolski and Ramstorf, 2002).

Acknowledgments

We are grateful to two anonymous reviewers for their critical and instructive comments on an early version of the manuscript. This work was supported by grants of National Nature Science Foundation of China (No.40631003, 40771009 and 40702026), The U.S. National Science Foundation (NSF ESH 0502535 to RLE and HC) and The Gary Comer Science and Education Foundation (CC8 and CP41 to RLE), Foundation of Creative Plan for Graduate Students of Jiangsu Province (NO. CX09B302Z).

Appendix. Supplementary information

Supplementary data associated with this article can be found in the online version, at doi:10.1016/j.quascirev.2010.01.008.

References

Ahn, J., Brook, E.J., 2007. Atmospheric CO_2 and climate from 65 to 30 ka B.P. Geophysical Research Letters 34, L10703. doi:10.1029/2007GL029551.
Alley, R.B., Clark, P.U., 1999. The deglaciation of the northern hemisphere: a global perspective. Annual Reviews of Earth and Planetary Sciences 27, 149–182.
Berger, A.L., 1978. Long-term variations of daily insolation and Quaternary climatic changes. Journal of the Atmospheric Sciences 35, 2362–2367.
Blunier, T., Brook, E.J., 2001. Timing of millennial-scale climate change in Antarctica and Greenland during the Last Glacial period. Science 291, 109–112.
Bond, G.C., Lotti, R., 1995. Iceberg discharges into the North Atlantic on millennial time scales during the Last Glaciation. Science 267, 1005–1010.
Bory, A.J.-M., Biscaye, P.E., Svensson, A., Grousset, F.E., 2002. Seasonal variability in the origin of recent atmospheric mineral dust at NorthGRIP, Greenland. Earth and Planetary Science Letters 196, 123–134.
Brauer, A., Haug, G.H., Dulski, P., Sigman, D.M., Negendank, J.F.W., 2008. An abrupt wind shift in western Europe at the onset of the Younger Dryas cold period. Nature GeoScience 1, 520–523.
Braun, H., Christl, M., Rahmstorf, S., Ganopolski, A., Mangini, A., Kubatzki, C., Roth, K., Kromer, B., 2005. Possible solar origin of the 1,470-year glacial climate cycle demonstrated in a coupled model. Nature 438, 208–211.
Broccoli, A.J., Dahl, K.A., Stouffer, R.J., 2006. Response of the ITCZ to Northern Hemisphere cooling. Geophysical Research Letters 33, L01702. doi:10.1029/2005GL024546.
Broecker, W.S., Bond, G., Klas, M., Bonani, G., Wolfli, W., 1990. A salt oscillator in the glacial Atlantic? 1. The concept. Paleoceanography 5, 469–477.
Broecker, W.S., 1998. Paleocean circulation during the Last Deglaciation: a bipolar seesaw? Paleoceanography 13, 119–121.
Carlson, A.E., LeGrande, A.N., Oppo, D.W., Came, R.E., Schmidt, G.A., Anslow, F.S., Licciardi, J.M., Obbink, E.A., 2008. Rapid early Holocene deglaciation of the Laurentide ice sheet. Nature GeoScience 1, 620–624.
Chappellaz, J.A., Fung, I.Y., Thompson, A.M., 1993. The atmospheric CH_4 increase since the Last Glacial Maximum. Tellus 45B, 228–241.
Cheng, H., Edwards, R.L., Wang, Y.J., Kong, X.G., Ming, Y.F., Kelly, M.J., Wang, X.F., Gallup, C.D., Liu, W.G., 2006. A penultimate glacial monsoon record from Hulu Cave and two-phase glacial terminations. Geology 34, 217–220.
de Abreu, L., Shackleton, N.J., Schönfeld, J., Hall, M., Chapman, M., 2003. Millennial-scale oceanic climate variability off the Western Iberian margin during the last two glacial periods. Marine Geology 196, 1–20.
Dickson, B., Yashayaev, I., Meincke, J., Turrell, B., Dye, S., Holfort, J., 2002. Rapid freshening of the deep North Atlantic ocean over the past four decades. Nature 416, 832–837.
Dorale, J.A., Liu, Z., 2009. Limitations of Hendy test criteria in judging the paleoclimatic suitability of speleothems and the need for replication. Journal of Cave and Karst Studies 71, 73–80.

EPICA Community Members, 2006. One-to-one coupling of glacial climate variability in Greenland and Antarctica. Nature 444, 195–198.
Firestone, R.B., West, A., Kennett, J.P., Becker, L., Bunch, T.E., Revay, Z.S., Schultz, P.H., Belgya, T., Kennett, D.J., Erlandson, J.M., Dickenson, O.J., Goodyear, A.C., Harris, R.S., Howard, G.A., Kloosterman, J.B., Lechler, P., Mayewski, P.A., Montgomery, J., Poreda, R., Darrah, T., Que Hee, S.S., Smith, A.R., Stich, A., Topping, W., Wittke, J.H., Wolbach, W.S., 2007. Evidence for an extraterrestrial impact 12,900 years ago that contributed to the megafaunal extinctions and the Younger Dryas cooling. Proceedings of the National Academy of Sciences of the United States of America 104, 16016–16021.
Ganopolski, A., Ramstorf, S., 2002. Abrupt glacial climate changes due to stochastic resonance. Physical Review Letters 88, 038501.1–038501.4.
Goodman, P., 2001. Thermohaline adjustment and advection in an OGCM. Journal of Physical Oceanography 31, 1477–1497.
Helmens, K.F., Bos, J.A.A., Engels, S., Van Meerbeeck, C.J., Bohncke, S.J.P., Renssen, H., Heiri, O., Brooks, S.J., Seppä, H., Birks, H.J.B., Wohlfarth, B., 2007. Present-day temperatures in northern Scandinavia during the Last Glaciation. Geology 35, 987–990.
Hemming, S.R., 2004. Heinrich events: massive late Pleistocene detritus layers of the North Atlantic and their global climate imprint. Reviews of Geophysics 42, RG1005. doi:10.1029/2003RG000128.
Hendy, C.H., 1971. The isotopic geochemistry of speleothems–I. The calculation of the effects of different modes of formation on the isotopic composition of speleothems and their applicability as palaeoclimatic indicators. Geochimca et Cosmochimica Acta 35, 801–824.
Hinnov, L.A., Schulz, M., Yiou, P., 2002. Interhemispheric space-time attributes of the Dansgaard–Oeschger oscillations between 100 and 0 ka. Quaternary Science Reviews 21, 1213–1228.
Hoerling, M.P., Hurrell, J.W., Xu, T.Y., 2001. Tropical origins for recent North Atlantic climate change. Science 292, 90–92.
Huber, C., Leuenberger, M., Spahni, R., Flückiger, J., Schwander, J., Stocker, T.F., Johnsen, S., Landais, A., Jouzel, J., 2006. Isotope calibrated Greenland temperature record over Marine Isotope Stage 3 and its relation to CH_4. Earth and Planetary Science Letters 243, 504–519.
IAEA/WMO, 2001. Global Network of Isotopes in Precipitation. Accessible at. The GNIP Database. http://isohis.iaea.org.
Indermühle, A., Monnin, E., Stauffer, B., Stocker, T.F., Wahlen, M., 2000. Atmospheric CO_2 concentration from 60 to 20 kyr BP from the Taylor Dome ice core, Antarctica. Geophysical Research Letters 27, 735–738.
Kaufman, A., Wasserburg, G.J., Porcelli, D., Bar-Matthews, M., Ayalon, A., Halicz, L., 1998. U-Th isotope systematics from the Soreq cave, Israel and climatic correlations. Earth and Planetary Science Letters 156, 141–155.
Kawamura, K., Nakazawa, T., Aoki, S., Sugawara, S., Fujii, Y., Watanabe, O., 2003. Atmospheric CO_2 variations over the last three glacial-interglacial climatic cycles deduced from the Dome Fuji deep ice core, Antarctica using a wet extraction technique. Tellus 55B, 126–137.
Kelly, M.J., Edwards, R.L., Cheng, H., Yuan, D.X., Cai, Y.J., Zhang, M.L., Lin, Y.S., An, Z.S., 2006. High resolution characterization of the Asian Monsoon between 146, 000 and 99, 000 years B.P. from Dongge Cave, China and global correlation of events surrounding Termination II. Palaeogeography, Palaeoclimatology, Palaeoecology 236, 20–38.
Kim, S.-T., O' Neil, J.R., 1997. Equilibrium and nonequilibrium oxygen isotope effects in synthetic carbonates. Geochimica et Cosmochimica Acta 61, 3461–3475.
Kudrass, H.R., Hofmann, A., Doose, H., Emeis, K., Erlenkeuser, H., 2001. Modulation and amplification of climatic changes in the Northern Hemisphere by the Indian summer monsoon during the past 80 k.y. Geology 29, 63–66.
Latif, M., 2001. Tropical Pacific/Atlantic Ocean interactions at multi-decadal time scales. Geophysical Research Letters 28, 539–542.
Li, C., Battisti, D.S., Schrag, D.P., Tziperman, E., 2005. Abrupt climate shifts in Greenland due to displacements of the sea ice edge. Geophysical Research Letters 32, L19702. doi:10.1029/2005GL023492.
Liu, Z., Otto-Bliesner, B.L., He, F., Brady, E.C., Tomas, R., Clark, P.U., Calson, A.E., Lynch-Stieglitz, J., Curry, W., Brook, E., Erickson, D., Jacob, R., Kutzbach, J., Cheng, J., 2009. Transient simulation of Last Deglaciation with a new mechanism for Bølling–Allerød warming. Science 325, 310–314.
Marshall, J., Dobson, F., Moore, K., Rhines, P., Visbeck, M., d'Asaro, E., Bumke, K., Chang, S., Davis, R., Fischer, K., Garwood, R., Guest, P., Harcourt, R., Herbaut, C., Holt, T., Lazier, J., Legg, S., McWilliams, J., Pickart, R., Prater, M., Renfrew, I., Schott, F., Send, U., Smethie, W., 1998. The Labrador Sea deep convection experiment. Bulletin of the American Meteorological Society 79, 2033–2058.
Mayewski, P.A., Meeker, L.D., Twickler, M.S., Whitlow, S., Yang, Q.Z., Lyons, W.B., Prentice, M., 1997. Major features and forcing of high-latitude northern hemisphere atmospheric circulation using a 110 000-year-long glaciochemical series. Journal of Geophysical Research 102, 26,345–26,366.
McManus, J.F., Oppo, D.W., Cullen, J.L., 1999. A 0.5-million-year record of millennial-scale climate variability in the North Atlantic. Science 283, 971–975.
Meese, D.A., Gow, A.J., Alley, R.B., Zielinski, G.A., Grootes, P.M., Ram, M., Taylor, K.C., Mayewski, P.A., Bolzan, J.F., 1997. The Greenland ice sheet project 2 depth-age scale: methods and results. Journal of Geophysical Research 102, 26,411–26,423.
Mickler, P.J., Stern, L.A., Banner, J.L., 2006. Large kinetic isotope effects in modern speleothems. Geological Society of America Bulletin 118, 65–81.
Mikolajewicz, U., Crowley, T.J., Schiller, A., Voss, R., 1997. Modelling teleconnections between the North Atlantic and North Pacific during the Younger Dryas. Nature 387, 384–387.
Monnin, E., Indermühle, A., Dällenbach, A., Flückiger, J., Stauffer, B., Stocker, T.F., Raynaud, D., Barnola, J.-M., 2001. Atmospheric CO_2 concentrations over the Last Glacial termination. Science 291, 112–114.
Munk, W., Dzieciuch, M., Jayne, S., 2002. Millennial climate variability: is there a tidal connection? Journal of Climate 15, 370–385.
Otterå, O.H., Drange, H., Bentsen, M., Kvamstø, N.G., Jiang, D., 2003. The sensitivity of the present-day Atlantic meridional overturning circulation to freshwater forcing. Geophysical Research Letters 30, 1898. doi:10.1029/2003GL017578.
Parrenin, F., Paillard, D., 2003. Amplitude and phase of glacial cycles from a conceptual model. Earth and Planetary Science Letters 214, 243–250.
Porter, S.C., An, Z.S., 1995. Correlation between climate events in the North Atlantic and China during the Last Glaciation. Nature 375, 305–308.
Rahmstorf, S., 1995. Bifurcations of the Atlantic thermohaline circulation in response to changes in the hydrological cycle. Nature 378, 145–149.
Rinterknecht, V.R., Clark, P.U., Raisbeck, G.M., Yiou, F., Bitinas, A., Brook, E.J., Marks, L., Zelčs, V., Lunkka, J.-P., Pavlovskaya, I.E., Piotrowski, J.A., Raukas, A., 2006. The Last Deglaciation of the southeastern sector of the Scandinavian ice sheet. Science 311, 1449–1452.
Romanov, D., Kaufmann, G., Dreybrodt, W., 2008. $\delta^{13}C$ profiles along growth layers of stalagmites: comparing theoretical and experimental results. Geochimica et Cosmochimica Acta 72, 438–448.
Ruth, U., Bigler, M., Röthlisberger, R., Siggaard-Andersen, M.-L., Kipfstuhl, S., Goto-Azuma, K., Hansson, M.E., Johnsen, S.J., Lu, H.Y., Steffensen, J.P., 2007. Ice core evidence for a very tight link between North Atlantic and East Asian glacial climate. Geophysical Research Letters 34, L03706. doi:10.1029/2006GL027876.
Schmittner, A., Appenzeller, C., Stocker, T.F., 2000. Enhanced Atlantic freshwater export during El Niño. Geophysical Research Letters 27, 1163–1166.
Shen, C.-C., Edwards, L.R., Cheng, H., Dorale, J.A., Thomas, R.B., Moran, S.B., Weinstein, S.E., Edmonds, H.N., 2002. Uranium and thorium isotopic and concentration measurements by magnetic sector inductively coupled plasma mass spectrometry. Chemical Geology 185, 165–178.
Sima, A., Paul, A., Schulz, M., 2004. The Younger Dryas-an intrinsic feature of late Pleistocene climate change at millennial timescales. Earth Planetary Science Letters 222, 741–750.
Spötl, C., Mangini, A., Richard, D.A., 2006. Chronology and paleoenvironment of Marine Isotope Stage 3 from two high-elevation speleothems, Austrian Alps. Quaternary Science Reviews 25, 1127–1136.
Steffensen, J.P., Andersen, K.K., Bigler, M., Clausen, H.B., Dahl-Jensen, D., Fischer, H., Goto-Azuma, K., Hansson, M., Johnsen, S.J., Jouzel, J., Masson-Delmotte, V., Popp, T., Rasmussen, S.O., Röthlisberger, R., Ruth, U., Stauffer, B., Siggaard-Andersen, M.-L., Sveinbjörnsdóttir, Á.E., Svensson, A., White, J.W.C., 2008. High-resolution Greenland ice core data show abrupt climate change happens in few years. Science 321, 680–684.
Stott, L., Poulsen, C., Lund, S., Thunell, R., 2002. Super ENSO and global climate oscillations at millennial time scales. Science 297, 222–226.
Stuiver, M., Grootes, P.M., 2000. GISP2 oxygen isotope ratios. Quaternary Research 53, 277–284.
Svendsen, J.I., Alexanderson, H., Astakhov, V.I., Demidov, I., Dowdeswell, J.A., Funder, S., Gataullin, V., Henriksen, M., Hjort, C., Houmark-Nielsen, M., Hubberten, H.W., Ingólfsson, Ó., Jakobsson, M., Kjær, K.H., Larsen, E., Lokrantz, H., Lunkka, J.P., Lyså, A., Mangerud, J., Matiouchkov, A., Murray, A., Möller, P., Niessen, F., Nikolskaya, O., Polyak, L., Saarnisto, M., Siegert, C., Siegert, M.J., Spielhagen, R.F., Stein, R., 2004. Late Quaternary ice sheet history of northern Eurasia. Quaternary Science Reviews 23, 1229–1271.
Svensson, A., Biscaye, P.E., Grousset, F.E., 2000. Characterization of late glacial continental dust in the Greenland ice Core project ice core. Journal of Geophysical Research 105, 4637–4656.
Svensson, A., Andersen, K.K., Bigler, M., Clausen, H.B., Dahl-Jensen, D., Davies, S.M., Johnsen, S.J., Muscheler, R., Parrenin, F., Rasmussen, S.O., Röthlisberger, R., Seierstad, I., Steffensen, J.P., Vinther, B.M., 2008. A 60000 year Greenland stratigraphic ice core chronology. Climate of the Past 4, 47–57.
Sy, A., Rhein, M., Lazier, J.R.N., Koltermann, K.P., Meincke, J., Putzka, A., Bersch, M., 1997. Surprisingly rapid spreading of newly formed intermediate waters across the North Atlantic Ocean. Nature 386, 675–679.
Timmermann, A., Okumura, Y., An, S.-I., Clement, A., Dong, B., Guilyardi, E., Hu, A., Jungclaus, J.H., Renold, M., Stocker, T.F., Stouffer, R.J., Sutton, R., Xie, S.-P., Yin, J., 2007. The Influence of a weakening of the Atlantic Meridional overturning circulation on ENSO. Journal of Climate 20, 4899–4919.
van Andel, T.H., 2002. The climate and landscape of the middle part of the Weichselian glaciation in Europe: the stage 3 project. Quaternary Research 57, 2–8.
Vellinga, M., Wood, R.A., 2002. Global climatic impacts of a collapse of the Atlantic thermohaline circulation. Climatic Change 54, 251–267.
Vidal, L., Labeyrie, L., van Weering, T.C.E., 1998. Benthic $\delta^{18}O$ records in the North Atlantic over the Last Glacial period (60–10 kyr): evidence for brine formation. Paleoceanography 13, 245–251.
Voelker, A.H.L., workshop participants, 2002. Global distribution of centennial-scale records for Marine Isotope Stage (MIS) 3: a database. Quaternary Science Reviews 21, 1185–1212.

Wang, B., Lin, H., 2002. Rainy season of the Asian-Pacific summer monsoon. Journal of Climate 15, 386–398.
Wang, X.F., Auler, A.S., Edwards, R.L., Cheng, H., Cristalli, P.S., Smart, P.L., Richards, D.A., Shen, C.-C., 2004. Wet periods in northeastern Brazil over the past 210 kyr linked to distant climate anomalies. Nature 432, 740–743.
Wang, X.F., Auler, A.S., Edwards, R.L., Cheng, H., Ito, E., Wang, Y.J., Kong, X.G., Solheid, M., 2007. Millennial-scale precipitation changes in southern Brazil over the past 90,000 years. Geophysical Research Letters 34, L23701. doi:10.1029/2007GL031149.
Wang, Y.J., Cheng, H., Edwards, R.L., An, Z.S., Wu, J.Y., Shen, C.-C., Dorale, J.A., 2001. A high-resolution absolute-dated Late Pleistocene monsoon record from Hulu Cave, China. Science 294, 2345–2348.
Wolff, E.W., Fischer, H., Röthlisberger, R., 2009. Glacial terminations as southern warmings without northern control. Nature GeoScience 2, 206–209.
Wu, J.Y., Wang, Y.J., Cheng, H., Edwards, L.R., 2009. An exceptionally strengthened East Asian summer monsoon event between 19.9 and 17.1 ka BP recorded in a Hulu stalagmite. Science in China Series D 52, 360–368.
Wunsch, C., 2006. Abrupt climate change: an alternative view. Quaternary Research 65, 191–203.
Yancheva, G., Nowaczyk, N.R., Mingram, J., Dulski, P., Schettler, G., Negendank, J.F.W., Liu, J.Q., Sigman, D.M., Peterson, L.C., Haug, G.H., 2007. Influence of the intertropical convergence zone on the East Asian monsoon. Nature 445, 74–77.
Yuan, D.X., Cheng, H., Edwards, R.L., Dykoski, C.A., Kelly, M.J., Zhang, M.L., Qing, J.M., Lin, Y.S., Wang, Y.J., Wu, J.Y., Dorale, J.A., An, Z.S., Cai, Y.J., 2004. Timing, duration, and transitions of the Last Interglacial Asian monsoon. Science 304, 575–578.